Hindawi
Advances in Condensed Matter Physics
Volume 2018, Article ID 9409583, 9 pages
https://doi.org/10.1155/2018/9409583

Research Article

A ROF Access Network for Simultaneous Generation and Transmission Multiband Signals Based on Frequency Octupling and FWM Techniques

Hui Zhou,[1] **Yunlong Shen**,[1] **Ming Chen**,[2] **Jun Cheng**,[1] **and Yuting Zeng**[1]

[1]*College of Information Science and Engineering, Hunan Normal University, Changsha 410081, China*
[2]*College of Physics and Information Science, Hunan Normal University, Changsha 410081, China*

Correspondence should be addressed to Hui Zhou; 232325252@qq.com

Received 14 May 2018; Accepted 8 July 2018; Published 2 September 2018

Academic Editor: Yan Luo

We report a radio-over-fiber (ROF) access network with multiple high-repetive frequency mm-wave signals generation utilizing a dual-parallel Mach-Zehnder modulator (DP-MZM) and an semiconductor optical amplifier (SOA) for multiple base stations (BSs). In the scheme, at the central station (CS), signal and pump with frequency interval of $8f_{RF}$ are generated by properly adjusting the parameters of the DP-MZM. After FWM in a SOA, new converted optical signals are obtained. Two tones of the optical signals are selected by using tunable optical filter (TOF), which are then sent into a photodiode (PD) to generate multiple mm-wave signals with different frequencies ($8f_{RF}$, $16f_{RF}$, and $24f_{RF}$) for different BSs. Based on the proposed scheme, the mm-wave signals with frequencies of 20, 40, and 60 GHz carrying 2.5 Gb/s signal by a 2.5GHz RF signal have been generated by numerical simulation. Simulation results show that the proposed ROF system architecture with multiple-frequency millimeter-wave signals generation serving multiple BSs can work well. This scheme can raise the capacity of ROF system, reduce the requirement of the repetitive frequency of the driven RF signal, and support multiple mm-wave wireless access for BSs.

1. Introduction

Radio-over-fiber (ROF) system has been considered a promising technology for supporting next generation broadband access networks since it can provide low transmission loss, wide bandwidth, immunity to radio-frequency (RF) interference, high flexibility, and enhanced microcell coverage [1–3]. In the ROF system, the functions of carrier modulation and multiplexing are centralized in the central station (CS), and the remote base stations share a central station. In the base station (BS), a simple photodiode is used to produce electric millimeter wave and then is transmitted to the user terminal for demodulation by a simple distributed antenna. Thus the system has simplified structure and high cost benefit. However, generation of mm-wave signal in the conventional electronic domain will meet electronic bottleneck, so an effective method to solve the problem is to produce mm-wave using microwave photonics technique.

At present, the methods of mm-wave signal generation in the optical domain include direct beating of a dual-wavelength laser at a PD [4]; optical mode-locked of the two laser diodes [5]; and optical external modulators technique [6]. Some methods presented to produce high-repetitive frequency optical mm-wave were reported previously [7–11]. Quadruple frequency mm-wave generation was already reported previously [7, 8] including frequency multiplication based on a dual-pump FWM scheme in nonlinear media [7], or using an optical modulator based on first-order sideband suppression and a silicon microresonator filter [8]. Octuple frequency mm-wave generation was reported by using multicascaded intensity modulators based on optical carrier suppression (OCS) scheme [9]. 16-tupling frequency mm-wave generation was proposed using two cascaded dual-parallel Mach-Zehnder modulators (DP-MZMs) [10]. 18 times frequency mm-wave generation has been proposed and demonstrated based on cascaded optical external modulators and FWM in SOA [11].

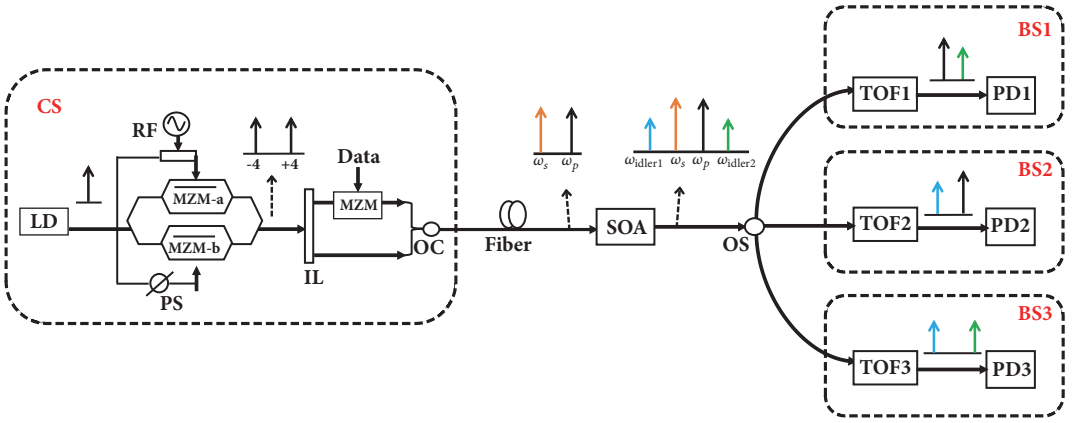

Figure 1: The principle of multiple-frequency optical mm-wave signals generation using DP-MZM and FWM in SOA for ROF system LD: laser diode, MZM: Mach-Zehnder modulator, OC: optical coupler, OS: optical splitter, SOA: semiconductor optical amplifier, TOF: tunable optical filter, and PD: photodio.

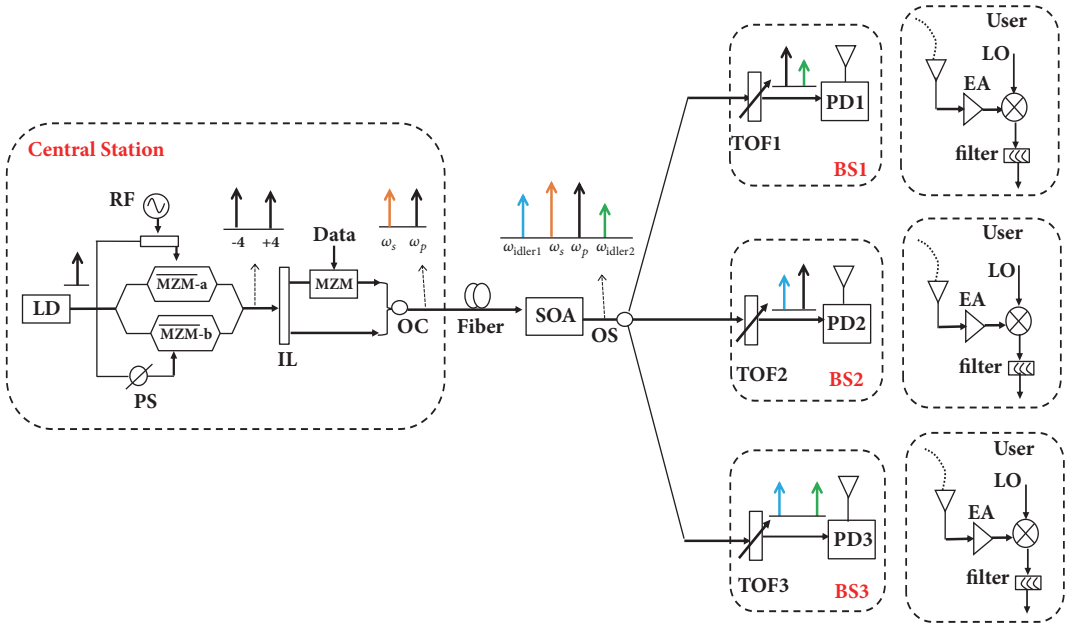

Figure 2: ROF architecture with multiband signals based on frequency octupling and FWM in SOA for multiple BSs.

Recently, some schemes for simultaneously generating multiband signals were reported [12–14]. Multiband signals generation including baseband, frequency-doubled, and frequency-quadrupled has proposed based on a dual-parallel Mach-Zehnder modulator, following a single-drive Mach-Zehnder modulator through optical carrier suppression and frequency-shifting techniques [12]. A scheme with multiband generation is proposed using two cascade MZMs to generate a DSB optical signal [13]. Anthoer scheme with multiband generation is proposed to generate an optical carrier suppression signal using two cascade MZMs [14]. However, the multiple high-repetitive frequency mm-wave signals generation for the ROF system is seldom reported, although it is considered very worthwhile for further studies.

In this paper, we propose a ROF system with 20GHz, 40GHz, and 60GHz based on based on frequency octupling and FWM techniques to providing multiband mm-wave wireless access. In our proposed multiband wireless accesses, a low frequency RF oscillator and a DP-MZM are required in the CS, which makes the CS cost-efficient. In our proposed multiband wireless accesses, since data is carried on one of the two sidebands, SSB like mm-wave format is transmitted over fiber, and amplitude fading and bit walk-off effect caused by chromatic dispersion are reduced greatly. Multiband mm-waves carrying same data are generated at BSs after beating frequency, which can provide the same data to every user.

This paper is organized as follows: the principle and theoretically analysis for the proposed multiband ROF access

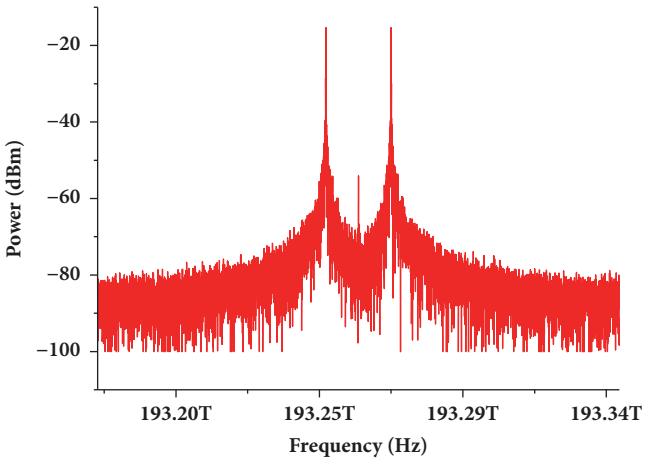

Figure 3: Optical spectrum after DP-MZM.

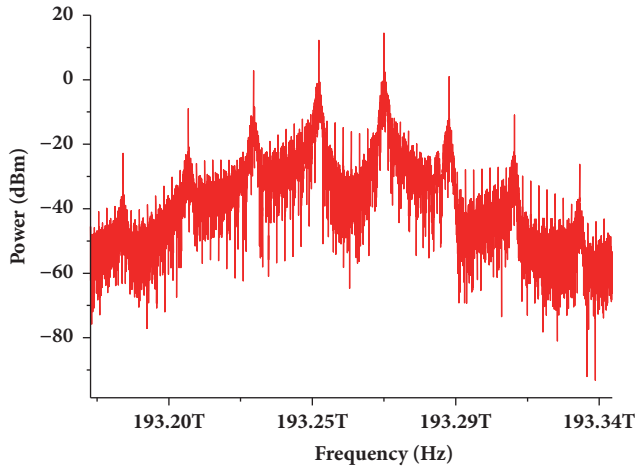

Figure 5: Optical spectrum after SOA.

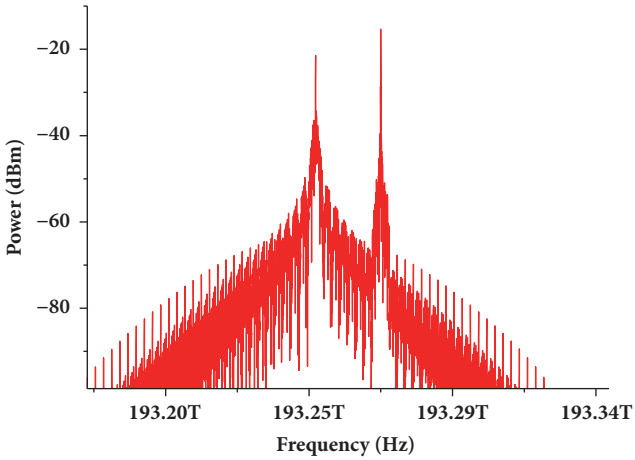

Figure 4: Optical spectrum after OC.

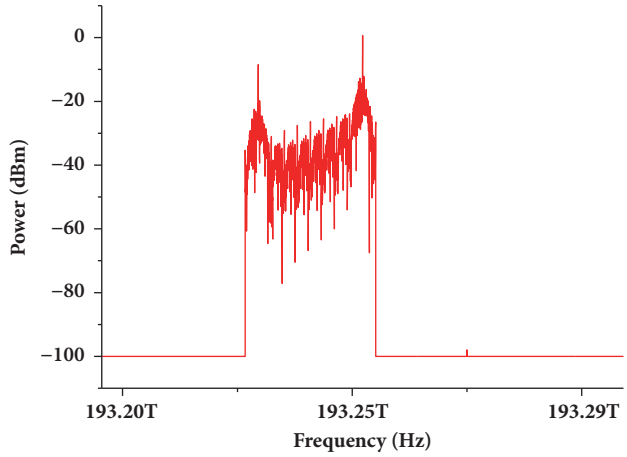

Figure 6: Optical spectrum of 20GHz mm-wave.

Network are presented in Section 2. In Section 3, a ROF system carrying 2.5Gbit/s NRZ signal supporting 20 GHz, 40 GHz, and 60GHz mm-waves access has been built to confirm the theoretical analysis. The conclusion is given in Section 4.

2. Theoretical Analysis

The principle of the proposed multiple-frequency millimeter-wave signals generation using DP-MZM and FWM in SOA for ROF system is shown in Figure 1. A continuous wave $E_{in}(t) = E_0 \cos(\omega_0 t)$ generated from an laser diode (LD) is injected into a DP-MZM, which consists of two sub-MZMs (MZM-a and MZM-b) in parallel. The two sub-MZMs are driven by the RF signal $V_{RF}(t) = V_{RF} \cos \omega_{RF} t$ with phase shift θ. The output optical from the MZM-a can be expressed as follows:

The output optical signal from the MZM-a can be described by

$$E_{out1}(t) = \frac{E_{in}(t)}{10^{(k/20)}} \left[\frac{1}{2} \exp\left(j\pi \frac{V_{RF} \cos(\omega_{RF} t)}{V_\pi} + j\pi \frac{V_{b1}}{V_{\pi DC}} \right) + \frac{1}{2} \exp\left(j\pi \frac{V_{RF} \cos(\omega_{RF} t + \theta)}{V_\pi} + j\pi \frac{V_{b2}}{V_{\pi DC}} \right) \right] \quad (1)$$

where E_0 and ω_0 are the amplitude and angle frequency of CW, V_{RF}, and ω_e are the amplitude and angle frequency of RF signal and k and V_π are the insertion loss and half-wave voltage of the sub-MZMs, respectively. V_{b1} and V_{b2} are the constant dc-bias voltages on the two arms of MZM. Assuming

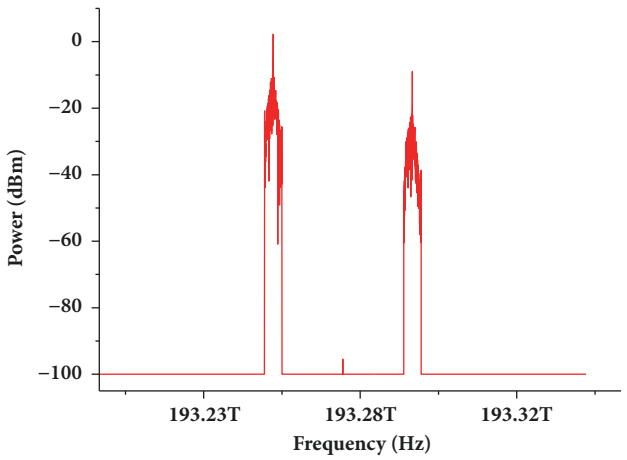

Figure 7: Optical spectrum of 40GHz mm-wave.

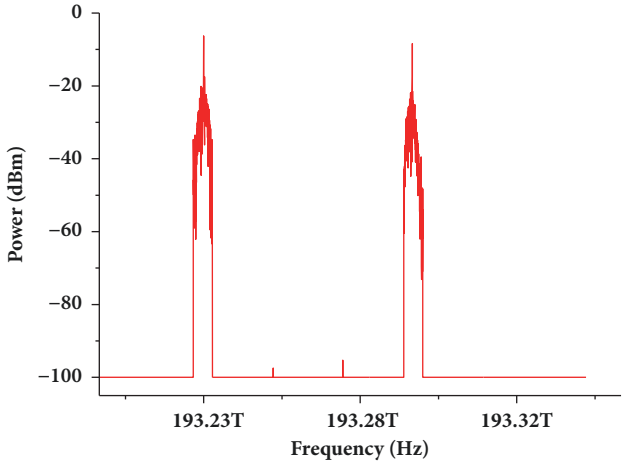

Figure 8: Electrical spectrum of 60GHz mm-wave.

$V_{b2} = 0$, the output optical signal from MZM-a can be expressed as

$$E_{out1}(t) = \frac{E_0(t)}{2}\left\{\cos\left(\omega_0 t + \frac{\pi V_{RF}}{V_\pi}\cos(\omega_{RF}t + \theta)\right) + \cos\left(\omega_0 t + \frac{\pi V_{RF}}{V_\pi}\cos\left(\omega_{RF}t + \frac{\pi V_{b1}}{V_\pi}\right)\right)\right\} \quad (2)$$

In a similar way to the MZM-a, the optical signal from MZM-b can be expressed as

$$E_{out2}(t) = \frac{E_0(t)}{2}\left\{\cos\left(\omega_0 t + \frac{\pi V_{RF}}{V_\pi}\cos(\omega_{RF}t + \theta + \phi)\right) + \cos\left(\omega_0 t + \beta\cos\left(\omega_{RF}t + \frac{\pi V_{b1}}{V_\pi} + \phi\right)\right)\right\} \quad (3)$$

where ϕ is the phase difference between the two sub-MZMs caused by RF signals. Assuming that $\beta = \pi V_{RF}/V_\pi$ is the modulation depth of the MZM, $\varphi = \pi V_{b1}/V_{\pi DC}$

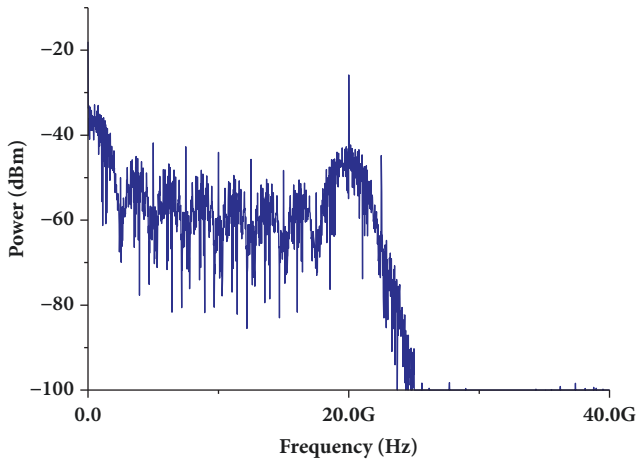

Figure 9: Electrical spectrum of 20GHz mm-wave.

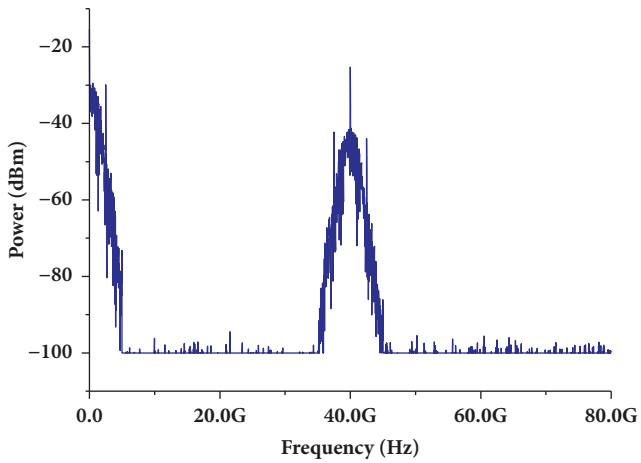

Figure 10: Electrical spectrum of 40GHz mm-wave.

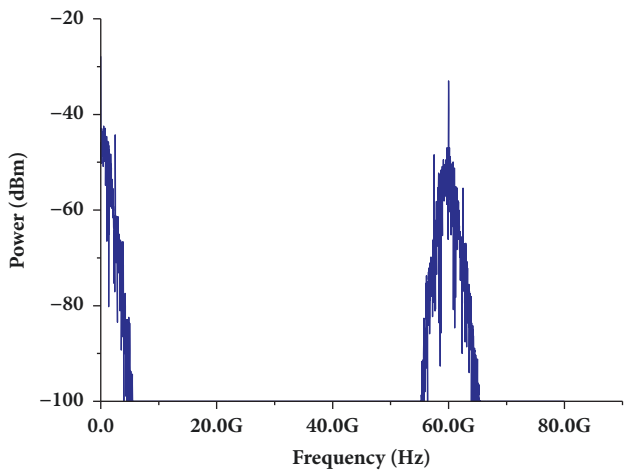

Figure 11: Electrical spectrum of 60GHz mm-wave.

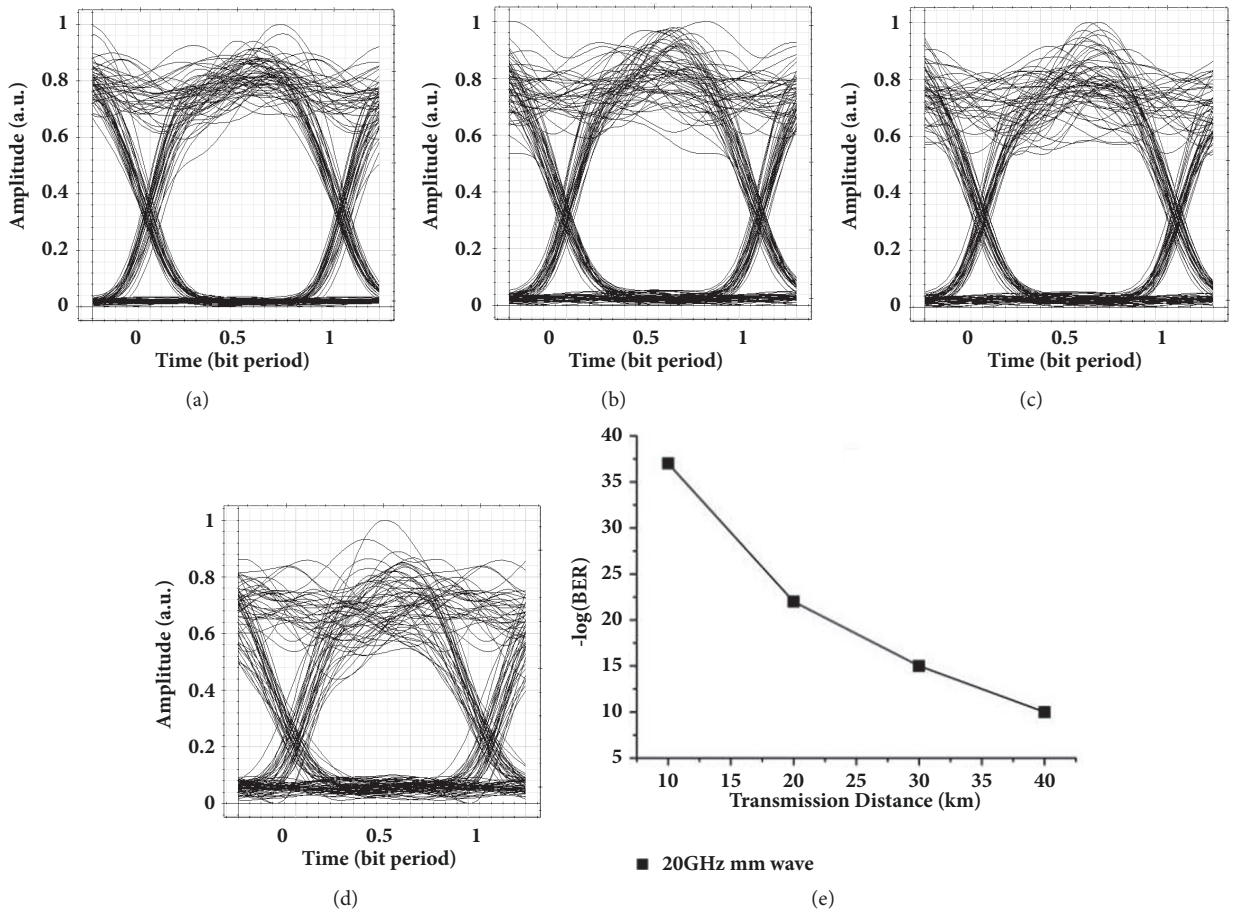

Figure 12: Baseband signal eye diagram of 20GHz mm-wave after fiber transmission over (a) 10 km, (b) 20 km, (c) 30 km, (d) 40 km, and (e) BER versus transmission distance.

is constant phase shift determined by the constant dc-bias voltage. The real part of (2) can be expressed as

$$E_{out1}(\mathrm{t}) = \frac{1}{2}E_0(t)\left\{\cos\left[\omega_0 t + \beta\cos\left(\omega_{RF}t + \theta\right)\right] + \cos\left[\omega_0 t + \beta\cos\left(\omega_{RF}t + \varphi\right)\right]\right\} \tag{4}$$

Likewise, the real part of (3) can be expressed as

$$E_{out2}(t) = \frac{1}{2}E_0(t)\left\{\cos\left[\omega_0 t + \beta\cos\left(\omega_{RF}t + \theta + \phi\right)\right] + \cos\left[\left(\omega_0 t + \beta\cos\left(\omega_{RF}t + \varphi + \phi\right)\right)\right]\right\} \tag{5}$$

When $\varphi = 0$, $\theta = \pi$, and $\phi = \pi/2$, based on Bessel function expansion of the output optical signals from MZM-a and MZM-b, (4) and (5) can be written as

$$E_{out1}(t) = E_0\cos\left(\omega_0 t\right) \cdot \left\{J_0(\beta) + 2\sum_{n=1}^{\infty}(-1)^n J_{2n}(\beta)\cos\left(2n\omega_{RF}t\right)\right\} \tag{6}$$

$$E_{out2}(t) = E_0\cos\left(\omega_0 t\right) \cdot \left\{J_0(\beta) + 2\sum_{n=1}^{\infty}(-1)^n J_{2n}(\beta)\cos 2n\left(\omega_{RF}t + \frac{\pi}{2}\right)\right\} \tag{7}$$

Here, J_n ($n = 0, 1\ldots$) denotes the nth order Bessel function of the first kind. From (6) and (7), it shows that the odd order sidebands are suppressed and the second-order sidebands are offset by the two branches (MZM-a and MZM-b), while the fourth-order sidebands are strengthen. When $\beta = 4.8$, according to the fourth-order Bessel functions of the first kind $J_4(\beta)$, the fourth-order sidebands have appreciable amplitude while the central carrier and higher-order sidebands have much small amplitudes. Two optical signals from two sub-MZMs are combined in the Y-branch of the DP-MZM. The output optical signal of the DP-MZM can be described as follows:

$$E_{out} = E_{out1}(\mathrm{t}) + E_{out2}(\mathrm{t}) = E_0 J_4(\beta)\left[\cos\left(\omega_0 - 4\omega_{RF}\right)t + \cos\left(\omega_0 + 4\omega_{RF}\right)t\right]. \tag{8}$$

Here, we assume that the signal is modulated on the sideband with the frequency of $\omega_s = \omega_0 - 4\omega_{RF}$ as signal lightwave and the sideband with the frequency of $\omega_p = \omega_0 +$

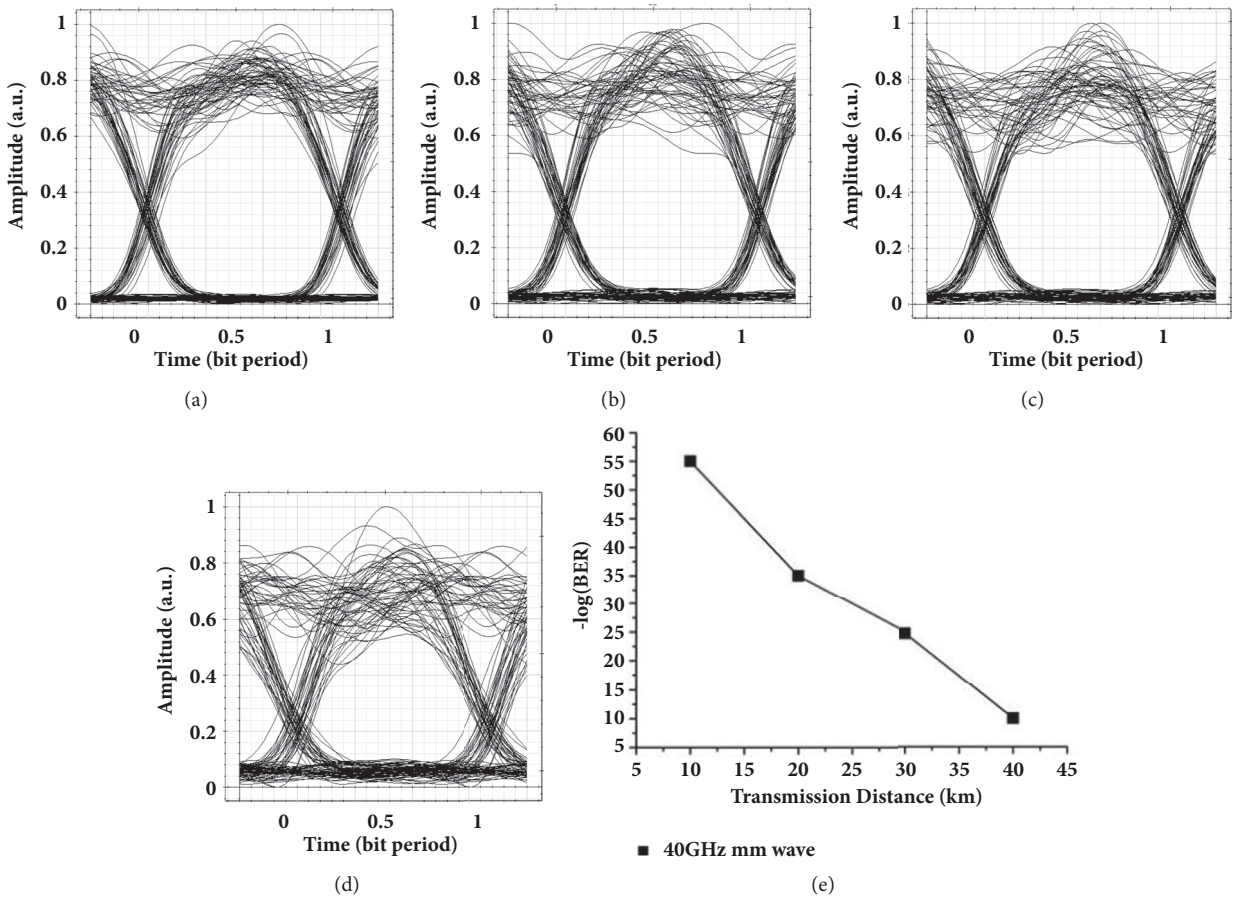

FIGURE 13: Baseband signal eye diagram of 40GHz mm-wave after fiber transmission over (a) 10 km, (b) 20 km, (c) 30 km, (d) 40 km, and (e) BER versus transmission distance.

$4\omega_{RF}$ is used as pump. The signal lightwave and pump are combined by an optical coupler and launched into a fiber. The combined optical signals are similar to SSB scheme, which suffer litter degration from fiber chromatic dispersion. After fiber transmission, the optical signals with the frequencie ω_s and ω_p input a SOA for four-wave mixing (FWM). According to the principle of FWM, pairs of input tones are imagined to beat to produce gain and phase gratings, which modulate or scatter the input fields to generate upper and lower sidebands [15]. Then two new converted signals with the frequency of $\omega_{ider1} = 2\omega_s - \omega_p$ and $\omega_{ider2} = 2\omega_p - \omega_s$ are generated. All optical signals with the frequencies ω_s, ω_p, ω_{ider1}, and ω_{ider2} from the SOA are divided into different branches for every BS by using an optical power splitter (OS). At each BS, two frequency components of the all optical sidebands are chosen by using tunable optical filter (TOF) and sent into a PD to generate a particular frequency mm-wave signal. In this scheme, there are four optical tones, and 6 groups of two tones combination such as $[\omega_s, \omega_p]$,$[\omega_s, \omega_{ider1}]$,$[\omega_s, \omega_{ider2}]$, $[\omega_p, \omega_{ider1}]$, $[\omega_p, \omega_{ider2}]$, and $[\omega_{ider1}, \omega_{ider2}]$ can be obtained. For example, the frequencies of ω_{ider1} and ω_s are chosen and are injected to a square-law photodiode (PD) to obtain the mm-wave signal with the frequency of $\omega_s - \omega_{ider1}$, namely, a millimeter wave with octupling of the RF signal generated. Similarly, filtered out $[\omega_p, \omega_{ider1}]$ or $[\omega_{ider1}, \omega_{ider2}]$ can also be used to produce the 16 times or even 24 RF signal mm-wave. For example, the frequencies of ω_s and ω_{ider1} are filtered out by TOF1, and the optical mm-wave signal with the frequency $\omega_s - \omega_{ider1}$ can be obtained, which can be expressed as

$$E_{out-BS1}(t) = d(t) E_0 J_4(\beta) \sqrt{G} \left[\cos\left(\omega_0 - 4\omega_{RF}\right) t + G E_0^2 J_4^2(\beta) r\left(8\omega_{RF}\right) \cos\left(\omega_0 - 12\omega_{RF}\right) t\right] \quad (9)$$

Here, G is the SOA' s gain and $r(8\omega_{RF})$ represent conversion efficiency coefficient [15]. When the optical mm-wave is detected by a PD, the photocurrent can be expressed as

$$I_{BS1}(t) = \mu \left|E_{out}(t)\right|^2 \approx \mu \left|d(t)\right|^2 E_0^4 J_4^2(\beta) r\left(8\omega_{RF} t\right) \cos\left(8\omega_{RF} t\right) \quad (10)$$

Here, μ is the conversion efficiency of the photon detector. From above, electric mm-wave with eightfold frequency of the RF signal is obtained. Similarly, when the optical mm-wave signals with $\omega_{ider2} - \omega_s$ and $\omega_{ider2} - \omega_{ider1}$ are filtered out

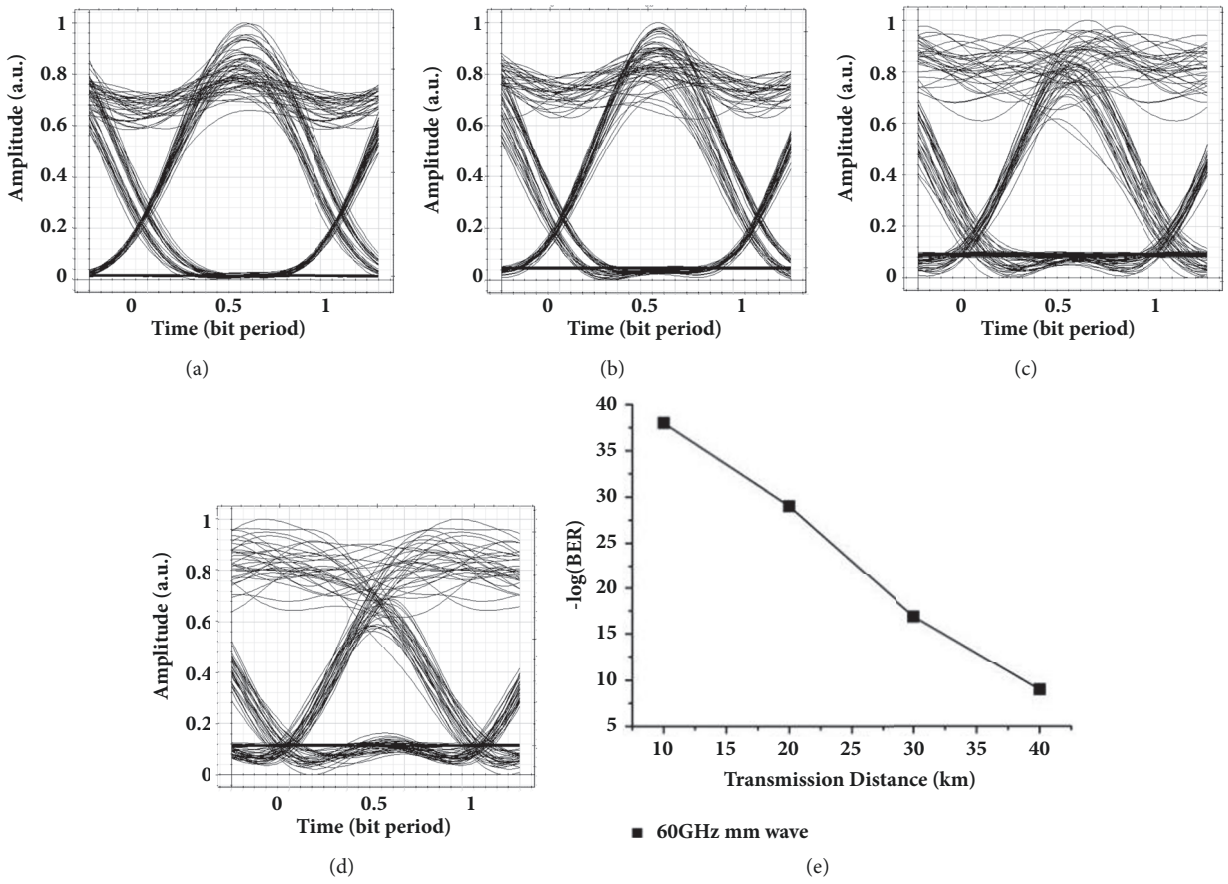

Figure 14: Baseband signal eye diagram of 60GHz mm-wave after fiber transmission over (a) 10 km, (b) 20 km, (c) 30 km, (d) 40 km, and (e) BER versus transmission distance.

and then are detected by PD, respectively, the photocurrents can be written as

$$I_{BS2}(t) = \mu \left|E_{out}(t)\right|^2 \approx \mu \left|d(t)\right|^2 E_0^4 J_4^2(\beta)\, r(8\omega_{RF}) \cos(16\omega_{RF} t) \quad (11)$$

$$I_{BS3}(t) = \mu \left|E_{out}(t)\right|^2 \approx \mu \left|d(t)\right|^2 E_0^4 J_4^2(\beta)\, r(8\omega_{RF}) \cos(24\omega_{RF} t) \quad (12)$$

Therefore, electric mm-waves with 16 times and 24 times RF frequency are obtained.

3. Simulation and Results

In order to verify our proposed scheme, the ROF architecture with multiband signals is built by OptiSystem, as shown is Figure 2. At the CS, the lightwave is generated from an external-cavity laser (ECL) at 193.26 THz with a 100 MHz linewidth, which is divided into two parts by an optical power splitter. The two parts are injected into dual-parallel Mach-Zehnder modulator (DP-MZM), respectively. The two sub-MZMs with the switching voltage of 4 V, insertion loss of 5dB, and extinction ratio of 80dB, respectively, are combined by two 3 dB couplers in parallel. According to theory presented in Section 2, the phase difference between the two arms of the sub-MZM is $\theta = \pi$ and two sub-MZMs are dc biased at the maximum optical output point ($\varphi = 0$). Two sub-MZMs are driven by a 2.5 GHz RF signal with $\phi = \pi/2$ phase shift and amplitude of 6.12 V (namely, $\beta = 4.8$). The output optical signal from the DP-MZM includes the lower and upper fourth-order sidebands at 193.25 THz and 193.27 THz, as shown in Figure 3. Then, an interleaver (IL) is used to separate the two fourth-order sidebands, and the 2.5Gbit/s NRZ baseband signal is modulated on the sideband 193.25 THz. The modulated signal lightwave coupled with pump by an optical coupler (OC) via fiber channel then sends to SOA. The optical spectrum after optical coupler is shown in Figure 4. The output signal is then amplified by an optical amplifier and the input power to fiber channel is about 0.8dBm. The SOA injection current is 0.32 A. The differential gain of SOA is 2.78×10^{-20} m^2, the initial carrier density is 3×10^{24} m^3, and the carrier density at transparent is 1.4×10^{24} m^3. In the SOA, new optical sidebands with different frequencies generated through the FWM effect and the optical spectrum after SOA are shown in Figure 5.

These optical signals are transmitted to the BSs, and any two different frequencies can be chosen using tunalble optical

filter (TOF), which can be sent into photodiode (PD) to generate electrical mm-wave. Figures 6–8 show the optical spectrum of mm-waves after the TOFs. The frequencies of 193.23THz and 193.25THz (ω_p and ω_{ider2}) were filtered out using TOF1 at the BS1, as shown in Figure 6. The frequencies of 193.25THz and 193.29THz (ω_{ider1} and ω_p) were filtered out using TOF2 at the BS2, as shown in Figure 7. The frequencies of 193.23THz and 193.29THz (ω_{ider1} and ω_{ider2}) were filtered out using TOF3 at the BS3, as shown in Figure 8. Figures 9–11 show the electrical spectrum of mm-waves after the PDs. As demonstrated in Figure 9, the mm-wave signal with the frequency $\omega_{ider2} - \omega_p = 8\omega_{RF}$, namely, mm-wave signal with the frequency of 20 GHz, has been obtained. Similarly, the mm-wave signal with the frequency $\omega_{ider1} - \omega_p = 16\omega_{RF}$, namely, mm-wave signal with the frequency of 40 GHz, has been obtained, as shown in Figure 10. The mm-wave signal with the frequency $\omega_{ider2} - \omega_{ider1} = 24\omega_{RF}$, namely, mm-wave signal with the frequency of 40 GHz, has been obtained, as shown in Figure 11. From Figures 9–11, we can see that the mm-wave signals with frequency of 20 GHz, 40 GHz, and 60 GHz have very high spectral purity. In the simulation, the peak power of the RF signal is dropped by almost 60dB after TOF and the reason is that a rectangular filter is used.

Figures 12–14 show the bit error rate (BER) and eye diagrams performances of the ROF system with the proposed multiple-frequency mm-wave signals generation at different fiber distances of BTB, 20 and 40 km. It shows that eyes become narrow as the distance increases, which is induced by the high-order chromatic dispersion and noise of the fiber, while the eye diagrams still remain open even after being transmitted over 40 km optical fiber. This proves that the proposed optical mm-wave signal does not suffer from the bit walk-off effect caused by the chromatic dispersion. The reason is that the data signal is modulated onto one optical tone and the other tone keeps constant amplitude and phase, so the bit walk-off effect is eliminated although the time delay difference between the two optical tones caused by the fiber dispersion increases linearly.

4. Conclusion

In this paper, a ROF system supporting multiband wireless access using frequency multiplication technique has been proposed and demonstrated. The proposed scheme utilizes a DP-MZM and an SOA. The signal and pump has been generated by properly adjusting the parameters of the DP-MZM. The coupled signal and pump through the fiber then input the SOA. In SOA, new converted signals are generated due to four-wave mixing effect. After optical filtering, two different frequencies can be chosen, which can be sent in to photodiode (PD) to generate the optical mm-wave with 8-tupling, 16-tupling, or 24-tupling of the RF signal frequency. The mm-wave signals with the frequencies of 20, 40, and 60 GHz by using 2.5GHz RF signal have been generated for different BSs by simulaiton, and eye diagrams performances of the 2.5 Gbit/s modulated signals have been measured.The simulation results show that the signals have good performance even after 40 km optical fiber transmission. Because the multiple-frequency mm-wave signals are generated adopting the proposed scheme, this method is a promising candidate to enhance the capacity of ROF system.

Data Availability

All data are included within the manuscript.

Conflicts of Interest

The authors declare that they have no conflicts of interest.

Acknowledgments

This work was partially supported by the National Natural Science Foundation of China (Grant nos. 61701180, 11647135, and 11704119), the Natural Science Foundation of Hunan Province (Grant nos. 2016JJ6097, 2017JJ3212, and 2018JJ3325), and Scientific Research Fund of Hunan Provincial Education Department (Grant nos. 17C0957, 17C0945).

References

[1] C. Lim, A. Nirmalathas, M. Bakaul et al., "Fiber-wireless networks and subsystem technologies," *Journal of Lightwave Technology*, vol. 28, no. 4, pp. 390–405, 2010.

[2] Y. Xiao and J. Yu, "Novel 60 GHz RoF system with optical single sideband mm-wave signal generation and wavelength reuse for uplink connection," *Optics Communications*, vol. 285, no. 3, pp. 229–232, 2012.

[3] Z. Jia, J. Yu, and G.-K. Chang, "A full-duplex radio-over-fiber system based on optical carrier suppression and reuse," *IEEE Photonics Technology Letters*, vol. 18, no. 16, pp. 1726–1728, 2006.

[4] J. Zhou, X. Feng, Y. Wang, Z. Li, and B.-O. Guan, "Dual-wavelength single-frequency fiber laser based on FP-LD injection locking for millimeter-wave generation," *Optics & Laser Technology*, vol. 64, pp. 328–332, 2014.

[5] Z. Deng and J. Yao, "Photonic generation of microwave signal using a rational harmonic mode-locked fiber ring laser," *IEEE Transactions on Microwave Theory and Techniques*, vol. 54, no. 2, pp. 763–767, 2006.

[6] J. Yu, Z. Jia, L. Yi, Y. Su, G.-K. Chang, and T. Wang, "Optical millimeter-wave generation or up-conversion using external modulators," *IEEE Photonics Technology Letters*, vol. 18, no. 1, pp. 265–267, 2006.

[7] . Jianjun Yu, . Ming-Fang Huang, . Zhensheng Jia, . Lin Chen, . Jian-Guo Yu, and . Gee-Kung Chang, "Polarization-Insensitive All-Optical Upconversion for Seamless Integration Optical Core/Metro/Access Networks With ROF Systems Based on a Dual-Pump FWM Scheme," *Journal of Lightwave Technology*, vol. 27, no. 14, pp. 2605–2611, 2009.

[8] J. Yu, Z. Jia, T. Wang, and G. K. Chang, "Centralized Lightwave Radio-Over-Fiber System with Photonic Frequency Quadrupling for High-Frequency Millimeter-Wave Generation," *IEEE Photonics Technology Letters*, vol. 19, no. 19, pp. 1499–1501, 2007.

[9] J. Lu, Z. Dong, L. Chen, J. Yu, and S. Wen, "High-repetitive frequency millimeter-wave signal generation using multi-cascaded external modulators based on carrier suppression technique," *Optics Communications*, vol. 281, no. 19, pp. 4889–4892, 2008.

[10] Z. Zhu, S. Zhao, X. Chu, and Y. Dong, "Optical generation of millimeter-wave signals via frequency 16-tupling without an optical filter," *Optics Communications*, vol. 354, pp. 40–47, 2015.

[11] T. Wang, H. Chen, M. Chen, J. Zhang, and S. Xie, "High-spectral-purity millimeter-wave signal optical generation," *Journal of Lightwave Technology*, vol. 27, no. 12, pp. 2044–2051, 2009.

[12] Q. Chang, H. Fu, and Y. Su, "Simultaneous generation and transmission of downstream multiband signals and upstream data in a bidirectional radio-over-fiber system," *IEEE Photonics Technology Letters*, vol. 20, no. 3, pp. 181–183, 2008.

[13] Z. Jia, J. Yu, Y.-T. Hsueh et al., "Multiband signal generation and dispersion-tolerant transmission based on photonic frequency tripling technology for 60-GHz radio-over-fiber systems," *IEEE Photonics Technology Letters*, vol. 20, no. 17, pp. 1470–1472, 2008.

[14] Y.-T. Hsueh, Z. Jia, H.-C. Chien, A. Chowdhury, J. Yu, and G.-K. Chang, "Multiband 60-GHz wireless over fiber access system with high dispersion tolerance using frequency tripling technique," *Journal of Lightwave Technology*, vol. 29, no. 8, pp. 1105–1111, 2011.

[15] J. P. R. Lacey, M. A. Summerfield, and S. J. Madden, "Tunability of polarization-insensitive wavelength converters based on four-wave mixing in semiconductor optical amplifiers," *Journal of Lightwave Technology*, vol. 16, no. 12, pp. 2419–2427, 1998.